https://doi.org/10.5194/egusphere-2026-256
Preprint. Discussion started: 2 March 2026

Combined and autonomous online measurement of water isotopes in precipitating snowflakes and atmospheric water vapor in East Antarctica

Thomas Lauwers[1,2], Elise Fourré[1], Niels Dutrievoz[1], Cécile Agosta[1], Olivier Jossoud[1], Bénédicte Minster[1], Frédéric Prié[1], Olivier Cattani[1], Valérie Masson-Delmotte[1], Mathieu Casado[1], Christophe Genthon[3], Amaëlle Landais[1]

[1]Laboratoire des Sciences du Climat et de l'Environnement – IPSL, UMR 8212, CEA-CNRS-UVSQ, Paris-Saclay University, Gif-sur-Yvette, France
[2]Météo-France, CNRS, Univ. Toulouse, CNRM, Toulouse, France
[3]Laboratoire de Météorologie Dynamique, Institut Pierre-Simon Laplace, Sorbonne Université/CNRS/École Polytechnique - IPP, Paris, France

Correspondence to: Thomas Lauwers (thomas.lauwers@meteo.fr)

Abstract. Water isotopes in precipitation are a powerful tool to better understand the processes governing snowfall in Antarctica, which is essential to improve our knowledge of the Antarctic atmospheric water cycle and surface mass balance, and for the interpretation of past climate signals archived in ice cores. However, precipitation isotope observations in Antarctica rely on manual sampling, which is prone to fractionation under low accumulation rates and remains both time-consuming and logistically demanding, and thus restricted to stations and seasons where manual sampling is feasible.

In this study, we present a novel method that enables autonomous, continuous, and combined measurements of water vapor and precipitation δD, using a single laser spectrometer. This technique offers new observational capabilities to better capture the isotopic signature of snowfall events in polar environments. Compared to conventional manual sampling of precipitation, the technique is capable of analysing very small amounts of condensed water, while avoiding post-depositional effects. In addition, it enables high-temporal-resolution observations and is well suited for long-term deployments in unmanned environments. The sampling system prototype has been deployed at Dumont d'Urville station, located on the coastal margin of East Antarctica, and evaluated during three precipitation events from February to June 2023. A dedicated post-processing algorithm was developed to retrieve the isotopic composition of precipitation from the surrounding vapor background. Comparisons with independently collected snow samples show a mean deviation of -5.4 ‰ in δD, which is well below the observed intra-event signal amplitude of about 100 ‰. This demonstrates the reliability of both the sampling system and the retrieval algorithm to study the isotopic composition of precipitation at the event-scale. With this new dataset, two applications are proposed to better understand the water vapor - precipitation relationship at Dumont d'Urville: (1) an evaluation of the LMDZ6iso general circulation model, and (2) a comparison with ground-based remote sensing instruments (ceilometer and micro rain radar) to explore the potential of the Δ(δD) metric as a proxy for snow formation altitude. Beyond polar applications,

https://doi.org/10.5194/egusphere-2026-256
Preprint. Discussion started: 2 March 2026

the proposed method opens new possibilities for other types of observations, including liquid precipitation sampling or cloud water isotopes monitoring onboard aircraft.

1 Introduction

Water isotopes are largely used for documenting the climate and water cycle since the first studies of Dansgaard in the 1950's (Dansgaard, 1954). The isotopic composition of water has been first analysed in precipitation (Ehhalt et al., 1963), snow (Gonfiantini and Picciotto, 1959; Lorius, 1961) and ice (Dansgaard et al., 1960). The isotopic ratio in precipitations can be linked to the temperature at high latitudes and to the quantity of precipitation (amount effect) at low latitudes (Dansgaard, 1964). The isotopic composition of water in precipitation can also provide constraints on the origin or climate conditions of the evaporative regions (Jouzel et al., 2013), moist air trajectories and mixing of water masses (Jouzel et al., 2013; Rozanski et al., 1982), and mean temperature in clouds, where snow is formed (Picciotto et al., 1960).

More recently, advances in laser spectroscopy have made possible the measurements of the isotopic composition of water vapor by instruments at ground or near ground level in several monitoring sites, with some observations lasting for several years (González et al., 2016; Guilpart et al., 2017; Leroy-Dos Santos et al., 2020, 2023; Noone et al., 2011; Steen-Larsen et al., 2013; Worden et al., 2007). The water vapor isotopic composition integrates the effect of phase changes along the atmospheric water cycle, thus providing added value for the understanding of the related processes. With these continuous vapor measurements, it is now possible to better identify effects such as evaporation over the ocean (Bonne et al., 2019), mixing of several air masses or re-evaporation (Landais et al., 2024), or exchange at the interface between snow and atmosphere (Steen-Larsen et al., 2013; Wahl et al., 2021).

In parallel with the increasing number of observations of the isotopic composition of water vapor and precipitation, several atmospheric general circulation models were equipped with water stable isotopes (Risi et al., 2010; Schmidt et al., 2007; Werner et al., 2011). Adding the water isotopes in the models permits to test and improve the representation of the atmospheric water cycle in the models. Pairing isotopic composition of water vapor and precipitations is also a strong added value for studying processes such as below cloud evaporation or mixing of air masses (Dütsch et al., 2016; Graf et al., 2019; Xing et al., 2023), while the additional use of cloud water isotopic measurement (Lowenthal et al., 2016, 2011) opens new insights into cloud processes (snow formation, riming, water vapor deposition). When coupled with remote sensing techniques, water isotopes can become powerful tools to improve our understanding of cloud microphysical processes (Muller et al., 2015; Weng et al., 2021).

Water isotopes are largely used in polar regions because their measurements in ice cores enable reconstructing the past temperature as well as patterns of the atmospheric water cycle. In Antarctica the longest continuous record of water isotopic composition was obtained on the EPICA Dome C ice core drilled at Concordia station (Jouzel et al., 2007). This record covers the last 800,000 years and depicts the climate variability on the orbital timescale (glacial – interglacial cycles lasting between 40,000 and 120,000 years), millennial timescale (Antarctic Isotopic Maxima during glacial periods) down to multi-decadal

https://doi.org/10.5194/egusphere-2026-256
Preprint. Discussion started: 2 March 2026

timescale (Grisart et al., 2022; Pol et al., 2014). Ice core recovery in more coastal regions with higher accumulation rate also permits to provide reconstructions at an annual scale (Emanuelsson et al., 2022; Jones et al., 2023).

The interpretation of the ice core records in Antarctica benefits more and more from water isotope enabled atmospheric general circulation models which can be evaluated using the isotopic composition of both precipitation and water vapor available at some stations (Bagheri Dastgerdi et al., 2021; Dutrievoz et al., 2025; Leroy-Dos Santos et al., 2023; Ollivier et al., 2025b). The relatively good agreement observed between modelled vapor and observations from the few equipped stations provides confidence in the model skills. Still, discrepancies remain, and in particular there is to our knowledge no study in which both water vapor and precipitation isotopic composition are well reproduced by the model outputs. Such mismatch is a limitation for the interpretation of water isotopic records in snow and ice in Antarctica.

Several explanations can be provided for the mismatch in the precipitation isotopic composition which can be linked to the representation or parameterization of the physical processes during precipitation formation and snow particle fall through the atmospheric column in polar region or simply to side effects of the sampling after a precipitation event. Indeed, under the influence of surface radiation and surface wind, the snow isotopic composition after a snowfall event can be rapidly obliterated by sublimation or metamorphism. This is the reason why samples are regularly discarded from the series of precipitation isotopic composition at Concordia because their weird isotopic values cast doubt on possible influence of post-deposition sublimation after the snowflake deposition on the sampling tables (Dreossi et al., 2024; Ollivier et al., 2025a).

We aim here at better describing the relationship between the isotopic composition of precipitation and the isotopic composition of water vapor and associated processes by getting rid of any influence of post-deposition processes between the snowfall event and the precipitation sampling. We thus present a new method enabling online measurements of the isotopic composition of falling snow near ground level in parallel to continuous isotopic measurements of the surrounding water vapor. We first present the instrumental setup deployed at the DDU station as well as the calculation for recovering the snowflake isotopic composition (Section 2). We then focus on a few precipitation events at DDU station to evaluate the accuracy of the new method (Section 3). Finally, we discuss the strengths and limitations of this new method and illustrate its potential to improve our understanding of the processes controlling the isotopic composition of precipitation in conjunction for instance with the use of general circulation model equipped with water isotopes or ground-based remote sensing observations (Section 4).

2. Methodology

2.1 Instrumental set-up

The instrumental set-up is composed of a Picarro analyser installed in 2018 (Leroy-Dos Santos et al., 2021) which has been continuously measuring atmospheric water vapor isotopes since then. During the austral summer season 22-23 the Picarro was moved to a new laboratory dedicated to atmospheric observations (ATMOS building) and a ProCEAS (AP2E company) laser spectrometer based on a new technology was installed as well (Lauwers et al., 2025). The calibration of the water isotopes

https://doi.org/10.5194/egusphere-2026-256
Preprint. Discussion started: 2 March 2026

analysers are performed with an updated version of the low-level humidity generator (LHLG) (Lauwers et al., 2025; Leroy-Dos Santos et al., 2021) also installed during the summer season 22-23.

In addition to water vapor isotopic composition measurement, the AP2E ProCEAS analyser was tested for combined, online measurement of the precipitation isotopic composition. For this purpose, a new sampling line was installed to capture snowflakes on the ATMOS building, as well as four additional electrovalves (V3 to V6) controlled by the LHLG software with a sequencer (Figure 1).

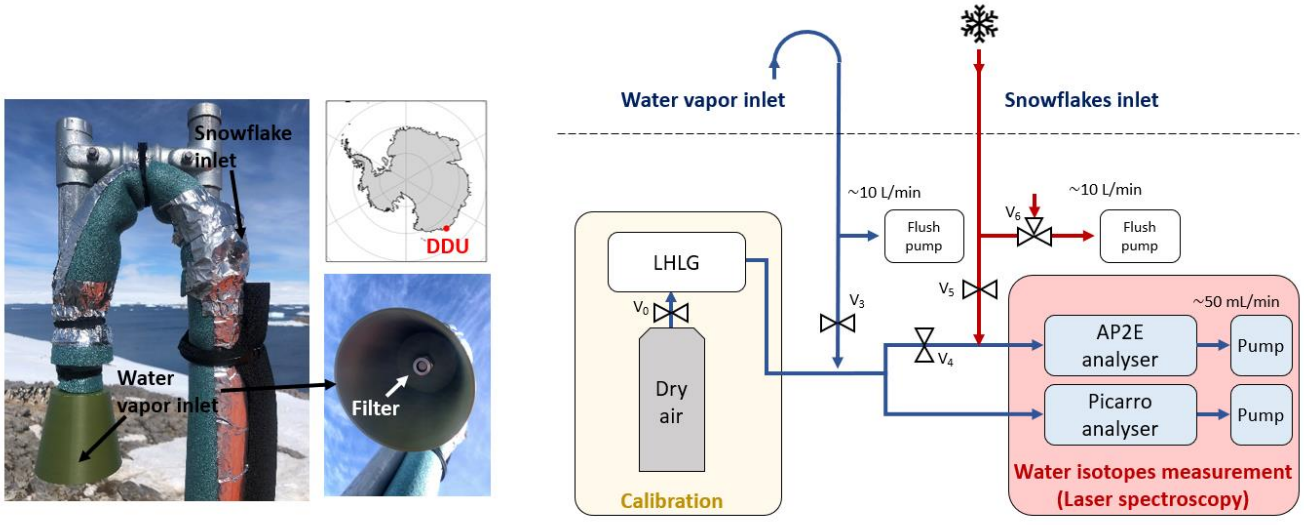

Figure 1: Sampling system. Left: photo of the 3 m sampling line installed on the ATMOS roof, showing the water vapor inlet (downward-facing, with a filter) and the snowflake inlet (upward-facing, 1/8″ aperture). The location of Dumont d'Urville Station (DDU) is indicated in the upper-right panel. Right: schematic of the full setup, including the external inlets, heated tubing, electrovalve system, calibration unit, and AP2E/Picarro laser spectrometers.

The 3 m sampling lines consists of two PFA tubes and a heating cord enclosed in an insulated sleeve, running from the roof of the ATMOS lab to the instruments inside. The first inlet ("water vapor inlet") is oriented downward and protected with a filter and cap to prevent snow intrusion. It is continuously flushed at 10 L min^{-1} by a KNF N96 pump and connected to both the Picarro and AP2E analysers for ambient water vapor measurements. The second inlet ("snowflake inlet") is oriented upward with a small aperture (1/8") to allow snowflakes to be pumped. Inside the heated tube, incoming snow particles are sublimated, and the vapor is drawn into the AP2E analyser. The four electrovalves, alternate between three operating states (Table 1). In the "Air" state, both analysers measure ambient vapor while both inlets are flushed at 10 L min^{-1}. Every 45 min, the system switches to the "Flake" state for 15 min: the Picarro instrument continues measuring ambient vapor, while the AP2E instrument is connected to the snowflake inlet, now carrying a mix of ambient vapor and sublimated snow. During this period, electrovalve V6 stops flushing the snowflake line so that 100% of the sublimated sample enters the analyser. Finally, every 46 hours, a calibration with two reference water isotopic standards is performed with the LHLG and lasts approx. 2 hours.

https://doi.org/10.5194/egusphere-2026-256
Preprint. Discussion started: 2 March 2026

State	Typical frequency	Picarro analyser	AP2E analyser	V3 (vapor inlet)	V4 (vapor AP2E)	V5 (snowflake inlet)	V6 (snowflake flush)
Air	45 min / h	Vapor		open	open	closed	open
Flake	15 min / h	Vapor	Vapor + Flake	open	closed	open	closed
Calibration	2 h / 2 d	Calibrated standard		closed	open	closed	open

Table 1: Description of the three operating states of the system ("Air," "Flake," "Calibration"), including the electrovalve configuration and typical frequency.

This configuration allows uninterrupted water vapor time series from the Picarro, while enabling the AP2E to measure precipitation and vapor in parallel.

2.2. Snow samples collection and measurement

During precipitation events throughout the year, snow is collected by winterover staff at high temporal resolution using two complementary methods: a wind sock mounted on a wind vane, which is able to capture snow associated with horizontal winds, and a 50 cm-deep tray which will preferentially collect vertically falling snow (Figure 2). At the onset of each event, both collection devices are emptied to avoid contamination from previous snow accumulation. The collected snow is then transferred into 50 mL Corning tubes, with a sampling period varying between 1 to 3 hours depending on the snowfall rate. To prevent mixing of snow over long periods and limit post-depositional processes such as sublimation, no sample was collected if the snow volume remained insufficient after three hours. This particular high-resolution sampling has been performed on a few selected events in 2023 to validate this study. Samples were stored at –20 °C at the station, then shipped to LSCE in refrigerated containers during the following austral summer.

The isotopic measurements were conducted at LSCE using a Picarro L2130-i spectrometer in liquid mode. The standard deviation of δD measurements (1σ) was 0.7‰, estimated from duplicate measurements on 15% of the samples ($\delta^{18}O$ measurements are not presented in this study; the reasons for this choice are detailed in the next section).

Figure 2: Manual snow collection setup. Left: sock mounted on a wind vane, designed to collect blowing snow. Right: open tray, preferentially capturing vertically falling snow.

https://doi.org/10.5194/egusphere-2026-256
Preprint. Discussion started: 2 March 2026

2.3. Water vapor isotopic composition correction

At DDU, the minimal ambient humidity is situated around 500 ppm (Leroy-Dos Santos et al., 2023), while maximal values can exceed 10 000 ppm in our setup, especially in the "flake inlet", when snowflake sublimation adds substantial water vapor. Current AP2E water isotope analysers are not optimized for such high humidity levels, as excessive optical absorption under these conditions can cause non-linearities. This "saturation" effect is particularly pronounced for $\delta^{18}O$, requiring specific spectral fitting procedures (Piel et al., 2024), while its impact on δD remains limited (Lauwers et al., 2025). Consequently, this study focuses on δD only.

Two main corrections are applied to the raw isotopic ratios given by the two spectrometers, already described in previous papers (Lauwers et al., 2025; Ollivier et al., 2025b):

- humidity dependency correction: a linear correction is accounted for the AP2E instrument (Lauwers et al., 2025). For the Picarro instrument, we account for a typical humidity dependency in the form of $f(h) = a_1/h + b_1 h + c_1$ (Weng et al., 2020), where h is the absolute humidity (in ppm). The reference humidity is fixed at 1000 ppm, for which the correction function is equal to 0. The corrected δD value reads $\delta D_{humcorr} = \delta D_{raw} - f(h)$. The parameters retrieved from the calibration are summed-up in Table 2.
- true value correction: correction parameters are retrieved from regular calibration data acquired during year 2023 at DDU with two VSMOW-SLAP calibrated standards FP5 (δD = - 394.7 ±-0.7‰) and AO1 (δD = -238.3 ±-0.7‰), at a reference humidity of 1000 ppm. The true value correction reads $\delta D_{true} = a_2 * dD_{humcorr} + b_2$, where $\delta D_{humcorr}$ is the isotopic composition corrected from the humidity dependency. The true value correction parameters are given in Table 2.

	Humidity dependency correction			**True value correction**	
	a_1 (‰.ppm)	b_1 (‰.ppm^{-1})	c_1 (‰)	a_2 (no unit)	b_2 (‰)
AP2E	0	$-2.7\ 10^{-3}$	2.7	1.01	-13.3
Picarro	1967.4	$1.4\ 10^{-3}$	-3.3	0.99	7.3

Table 2: Humidity dependency and true value correction parameters for both AP2E and Picarro spectrometers.

2.4 Retrieval of the isotopic composition of precipitation

Let us assume atmospheric water vapor of absolute humidity $h_v(t)$ and isotopic composition $\delta_v(t)$ (in oxygen 18 or deuterium), hereafter denoted "background water vapor". When a snowflake sublimates, its isotopic composition δ_p is diluted in the surrounding water vapor, resulting in a mixing between the snow sample and the background, with a total humidity $h_{mix}(t)$ and isotopic composition $\delta_{mix}(t)$.

To reconstruct the isotopic composition of the sublimated snow sample δ_p, we apply the formulation proposed by (Affolter et al., 2014) for calculating the isotopic composition of liquid water inclusions in speleothems:

https://doi.org/10.5194/egusphere-2026-256
Preprint. Discussion started: 2 March 2026

$$\delta_p = \frac{\overline{\delta_{mix}}\,\overline{h_{mix}} - \overline{\delta_v}\,\overline{h_v}}{\overline{h_{mix}} - \overline{h_v}} = \frac{\overline{\delta_{mix}}\,\overline{h_{mix}} - \overline{\delta_v}\,\overline{h_v}}{h_p} \quad (1)$$

Here the horizontal bar denotes the integrated value across time of both the humidity and the isotopic composition, the latter being weighted by the humidity value. Their values are calculated as follow:

$$\overline{\delta_j} = \frac{\int \delta_j(t) h_j(t) dt}{\int h_j(t) dt} \text{ and } \overline{h_j} = \frac{\int h_j(t) dt}{\int dt} \quad (2)$$

Where j refers to the "mix" or "background vapor" sequence. The main challenge in the retrieval of the snow isotopic composition lies in defining the integration limits, i.e. the precise start and end of each sequence. In the ideal configuration of (Affolter et al., 2014), water inclusions are injected in the laboratory into a stable "background" with constant humidity and isotopic composition. This is not the case here, as our background corresponds to atmospheric water vapor, which varies continuously over time. In addition, the laboratory setup allows precise control of the water flux from the inclusion, averaging over long periods with typical volumes around 1 µL. By contrast, the water content of an individual snowflake can vary widely, from a few µL down to ~ 0.01 µL, depending on particle size and shape (Leinonen et al., 2021).

As an example, Figure 3 shows the humidity and δD signal recorded on 16 April 2023 between 15:00 and 18:30 UTC. To minimize memory effects and artifacts (e.g., pressure fluctuations after valve switching), the first 4 minutes following each switch are discarded to calculate the isotopic composition of the precipitation δD_p (computed from Eq 1). In order to keep only reliable precipitation data, we also discard snowflake events when the sublimation mixing ratio $h_p/\overline{h_v}$ is situated below 10%. In the example shown on Figure 3, the last segment between 17:30 and 18:00 is not interpreted as a snowflake event and thus does not display any isotopic composition.

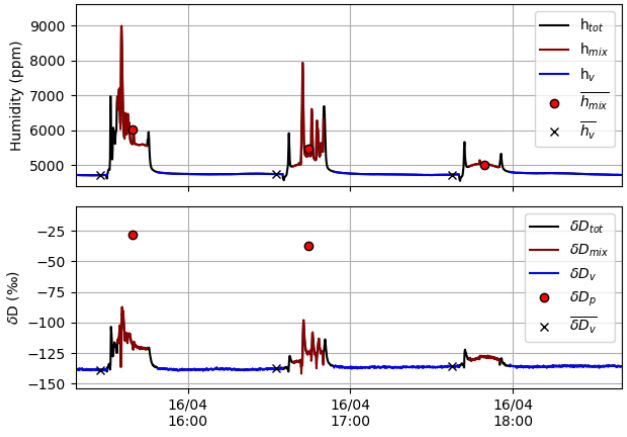

Figure 3: Example time series from AP2E analyser showing absolute humidity (top) and δD (bottom). Blue lines correspond to the "vapor" state (40 min), red lines to the "flake" state (11 min), black lines indicate artefacts excluded from analysis (4 min duration, due to valve switching). Black crosses show the mean of the last 5 min of each vapor segment for the humidity ($\overline{h_v}$) and δD ($\overline{\delta D_v}$) used for the background correction. The red circles show average humidity during the flake phase ($\overline{h_{mix}}$, top) and the retrieved isotopic composition of precipitation corrected from background vapor (δD_p, bottom).

https://doi.org/10.5194/egusphere-2026-256
Preprint. Discussion started: 2 March 2026

3. Results

3.1. Water vapor and precipitation measurements

This section presents the isotopic composition of water vapor and precipitation measured during three precipitation events at Dumont d'Urville (DDU) station in 2023, covering summer (21–24 February, mean temperature of -4.4°C), mid-season (14–19 April, mean temperature of -7.0°C), and winter (20–25 June, mean temperature of -15.8°C), selected to evaluate the sampling method under varying meteorological conditions. In addition, these events feature continuous snowfall during a relatively long period (24-48 hours) at high snowfall rate, enabling to make high frequency manual sampling (every 2 hours) with negligible post-deposition sublimation.

All three events display similar characteristics (Figure 4): a sharp increase in humidity (by a factor of ~2) marks the start of the precipitation event, followed by a sustained high-humidity phase lasting ~24 - 48 hours, and a gradual return to pre-event level as precipitation stops. This humidity evolution is accompanied by an initial enrichment in δD of the vapor, followed by a relatively high value during the event, and a subsequent decrease concomitant with the decline in humidity. The values obtained with the AP2E Proceas instrument both for humidity and isotopic composition are completely in line with the Picarro values, the latter instrument serving as reference. The δD of precipitation (both δD_p and δD_{cp}) is consistently enriched relative to the vapor and exhibits significant intra-event variability, with rapid changes reaching ~100 ‰ within approximately 3 hours, as observed in Figure 4b.

The three case studies demonstrate that the online measurements of δD_p show an overall very good agreement with the collected snow samples, both in terms of variability and absolute values, which validates our methodology. The next section focuses on the evaluation of the signal variability of the retrieved δD_p and an evaluation of its accuracy against the reference collected snow samples.

https://doi.org/10.5194/egusphere-2026-256
Preprint. Discussion started: 2 March 2026

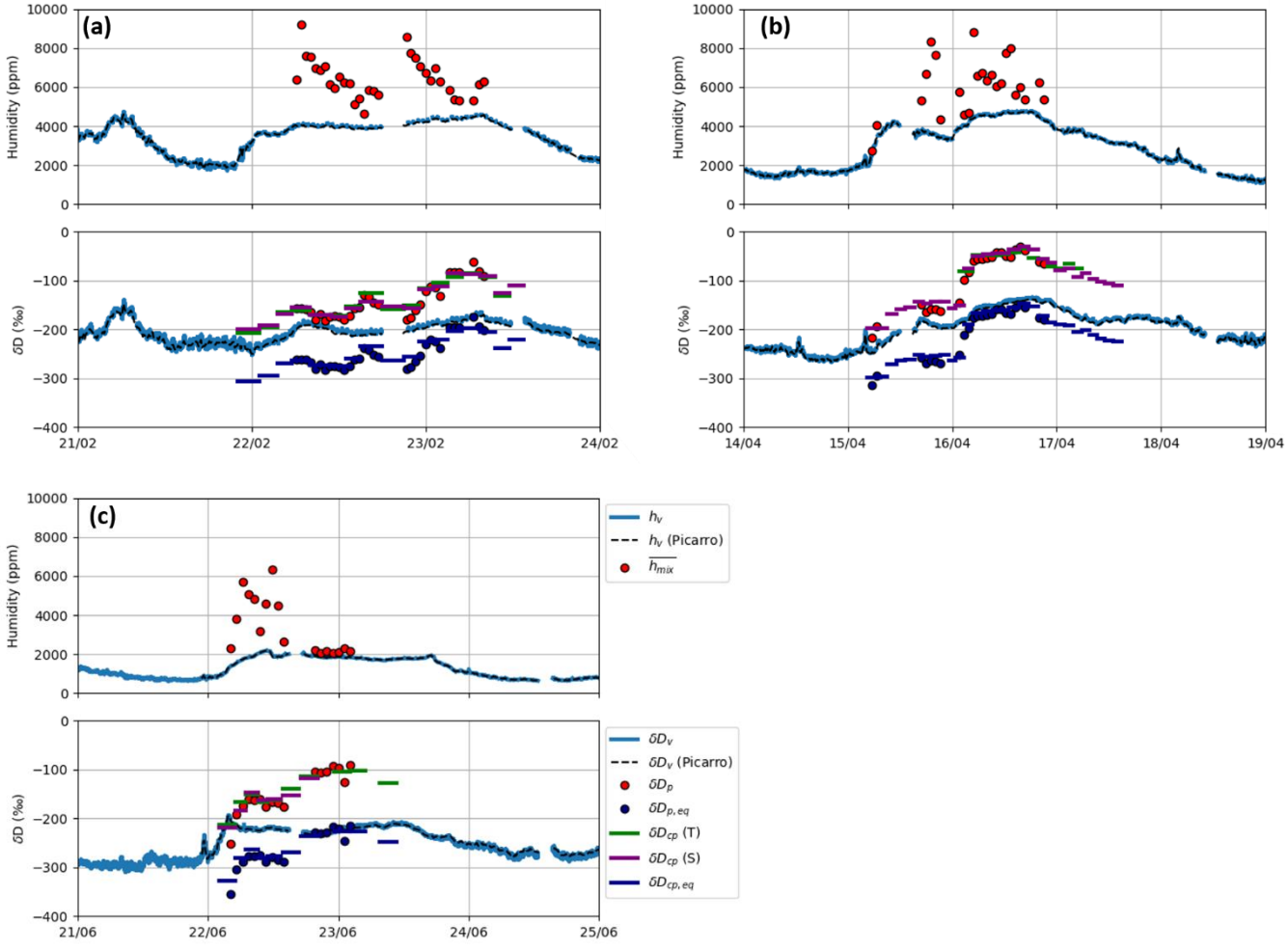

Figure 4: Isotopic measurements during the three selected precipitation events (a–c). Upper panels: water vapor mixing ratio from AP2E vapor inlet (h_v, blue line), snowflake inlet ($\overline{h_{mix}}$, red circles), and Picarro reference (black dashed line). Lower panels: δD of vapor (δD_v, blue line), computed online δD of precipitation (δD_p, red circles), δD of manually collected samples (δD_{cp}, horizontal lines; purple : windsock, green : tray; the length of the lines corresponds to the time between two sample collections) and Picarro reference for δD_v (black dashed line). Blue dots and blue horizontal lines indicate the isotopic composition $\delta D_{p,eq}$ and $\delta D_{cp,eq}$ of a theoretical vapor that would be in equilibrium with the precipitation (section 4.2). The gaps in the curves correspond to periods of automatic instrument calibration.

3.2. Precipitation isotopic signal variability and accuracy of the measurement technique

3.2.1. Signal variability

(Affolter et al., 2014) showed that differences in isotopologue diffusivities during liquid evaporation in their setup produce a characteristic asymmetric δD signal: an initial depletion (preferential evaporation of lighter isotopes), followed by enrichment after the humidity peak, and a return to background values. A similar kinetic effect occurs when snow or ice particles sublimate inside the heated sampling line. In addition, mixing of individual sublimated particles within the line complicate the signal.

https://doi.org/10.5194/egusphere-2026-256
Preprint. Discussion started: 2 March 2026

Together, these processes generate an instrumental short-term variability within a single flake phase (typically 15 min), governed by both isotopologue diffusivity and line properties (e.g., tubing volume, airflow, material). Finally, individual snowflakes may exhibit different isotopic compositions due to variations in their size, shape, and formation history (Del Guasta, 2022; Leinonen et al., 2021). This inter-snowflake variability could also contribute to short-term isotopic fluctuations observed within a single flake phase (~15 min), in addition to the instrumental effects mentioned above. As these contributions cannot be distinguished with our measurement setup, the resulting short-term variability is treated as noise and reduced through temporal integration.

We illustrate the effect of temporal integration with case 2 (Fig. 5), where δD was calculated with three integration times within the 15 min flake phase (excluding the first 4 min to minimize memory effects): 11 min, 4 min, and 1 min. The comparison highlights that shorter integrations yield much larger dispersion, demonstrating that averaging over more than 4 min is required to reduce uncertainty and obtain a robust isotopic composition.

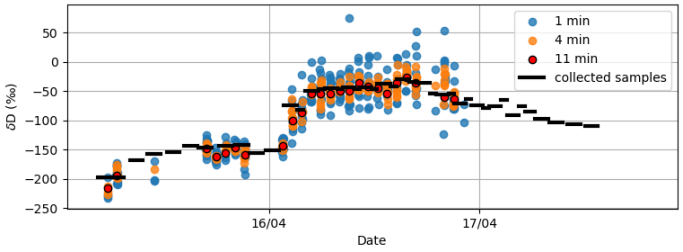

Figure 5: Sensitivity of retrieved δD_p to integration time for case 2. δD_p is calculated for three integration times within the 15 min flake phase (excluding first 4 min): blue dots show the 11 successive 1-min samples, orange dots the 7 overlapping 4-min samples (1-min step), and the red dot the 11-min integration. Black horizontal lines show reference δD from collected snow samples.

3.2.2. Estimation of the accuracy from collected snow comparison

In this section we use the collected snow samples as a reference to evaluate the precision and the accuracy of the online sampling dataset δD_p. For a quantitative evaluation, an interpolation is needed because the two datasets have very different sampling times. For example, during case 2 (see Figure 5) the online samples last 11 minutes and are performed every 45 minutes, while the manual sampling (snow collection) lasts 2 to 3 hours with no "dead-time" between each sample. We chose here to associate a discrete time for the manual sampling centred between the start and the end of the collection. If snow is collected at the same time with the tray or the wind sock, we average the isotopic composition to obtain one δ-value. The interpolated dataset $\delta D_{p,i}$ (diamonds) is obtained by weighting the δ by the amount of water of the corresponding sample (given by $h_p = \overline{h_{mix}} - \overline{h_v}$). Interpolation is performed only when there are at least two online samples within the 2–3 h manual snow collection interval, or when a single sample is available within 1 h of the snow collection time. Otherwise, no interpolation is applied to avoid biases caused by under sampling (e.g. during automatic calibration periods).

https://doi.org/10.5194/egusphere-2026-256
Preprint. Discussion started: 2 March 2026

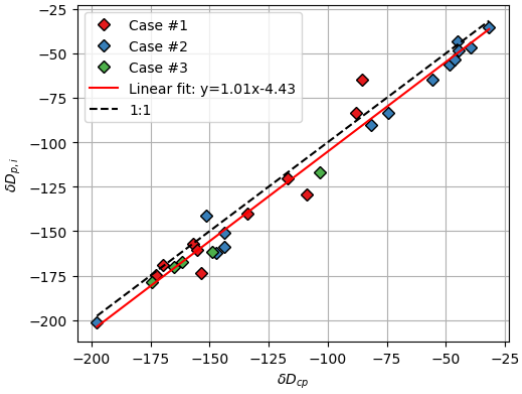

Figure 6: Comparison between the (interpolated) online precipitation isotope measurement $\delta D_{p,i}$ and the collected samples δD_{cp} (colored diamonds). The black dashed line shows the 1:1 reference; the red line shows the linear fit over the three case studies.

Figure 6 presents the comparison between the interpolated online measurements and the reference snow samples. The data exhibit a near 1:1 linear relationship, with an accuracy of -5.4 ‰ and a precision of 8.2 ‰. Here, accuracy is defined as the mean deviation between the collected precipitation samples δD_{cp} and the interpolated online measurements $\delta D_{p,i}$, while precision corresponds to the standard deviation of the linear regression residuals. Considering that the three events display typical δD_p variations of the order of 100 ‰ (see Figure 4), this level of accuracy and precision is sufficient to resolve detailed and quantitative variations at the intra-event scale.

4. Discussion

4.1. Instrumental and methodological aspects of *online* snowflake collection and isotope analysis

4.1.1. Optimal sampling frequency

Two key parameters must be tuned: the duration of the "flake" phase Δt_{flake} and the duration of the "vapor" phase Δt_{vap}. This tuning involves several requirements which affect the final results:

- Capture efficiency: longer Δt_{flake} increases the likelihood of intercepting snowflakes under low-precipitation conditions.
- Noise reduction: longer Δt_{flake} averages out short-term humidity and isotopic signal variability.
- Memory effect removal: shorter Δt_{flake} and longer Δt_{vap} helps flush the line and reduces residual contributions from previous snowflakes sublimation in the snowflake line.
- Temporal resolution: shorter Δt_{vap} enables description of rapid shifts in precipitation isotopic composition and identification of underlying processes.

https://doi.org/10.5194/egusphere-2026-256
Preprint. Discussion started: 2 March 2026

In practice, the proposed compromise of 15 min for Δt_{flake} and 45 min for Δt_{vap} provides stable results at Dumont d'Urville: this setting reduces measurement noise, sufficiently flushes the flake line while keeping a temporal resolution of 1 h. These parameters, however, should be adapted to location and meteorological context. For instance, continental plateau sites may benefit from more balanced settings (e.g. 20 min / 20 min), while very intense coastal snowfall events may require shorter Δt_{flake} and longer Δt_{vap} (e.g. 5-10 min flake / 50 min vapor) to avoid saturation in the sampling line, albeit at the cost of increasing measurement uncertainty. Finally, as observed in section 3.1 (Figure 4), δD_p can vary by up to 100 ‰ within a few hour. Integration times must therefore be long enough to average out noise, yet short enough to capture intra-event variability, which occurs on hourly timescales in the three cases presented.

4.1.2. Benefits, limitations, and future improvements

The method presented here offers several clear advantages. It operates autonomously, both day and night, without requiring human intervention. Moreover, the high temporal resolution achieved surpasses what is typically possible with manual sampling techniques. This autonomy is especially valuable for long-term deployments in remote environments where human intervention is impossible, and in particular for observation on the East Antarctic plateau where the precipitation events are rare and precipitation amounts are very small and where sublimation may affect the manual sampling (Ollivier et al., 2025a). The resulting high temporal resolution is unprecedented and could facilitate the evaluation of isotope-enabled atmospheric models and improve our understanding of atmospheric processes. Finally, the method could be extended to liquid precipitation sampling, or adapted for airborne campaigns to enable real-time measurements of cloud water.

Despite these advantages, two main limitations of the set-up presented in this work mainly concern the evaluation of $\delta^{18}O$ at high humidity, and the sampling representativity. First, $\delta^{18}O$ is difficult to measure in coastal areas with AP2E analysers because the $H_2{}^{18}O$ absorption peak is saturated at high humidity (Lauwers et al., 2025). The absence of $\delta^{18}O$ for this particular dataset prevents us from studying second order parameters such as d-excess, which gives additional information about out of equilibrium processes (Dreossi et al., 2024; Ollivier et al., 2025a). Second, the snow sampling representativity is not always guaranteed. Collection efficiency depends on wind direction and precipitation intensity: during certain periods no snowflakes enter the inlet despite ongoing precipitation (e.g., the second phase of the April 17 event, Figure 5), whereas under intense snowfall the inlet may flood. In addition, the small inlet diameter (1/8") may bias the collected particle size distribution.

Several improvements could enhance the system's performance and help overcome current limitations. For the collection, an adjustable diaphragm combined with an orientable inlet mounted on a wind vane could increase the probability of capturing snowflakes while regulating the vapor flux from snowflake sublimation. The diaphragm could be nearly closed during intense snowfall to avoid $\delta^{18}O$ saturation, and fully opened when precipitation is weak. On the software side, future developments could include an autonomous real-time adjustment of the vapor/snow sampling frequency to meet the requirements specified in Sect. 3.1.1. Finally, for very humid sites such as DDU in summer, replacing the AP2E with a Picarro analyser could enable

https://doi.org/10.5194/egusphere-2026-256
Preprint. Discussion started: 2 March 2026

robust measurements of both $\delta^{18}O$ and δD in precipitation since the CRDS technology is less affected by high humidity saturation. Higher temporal resolution could also be achieved by dedicating one analyser exclusively to snowflake measurements while the other continuously monitors water vapor. In this configuration, only occasional flushing of the snowflake line would be required, reducing memory effects and uncertainties linked to short integration times, while providing a continuous high-resolution precipitation dataset. Such a dual-analyser setup requires however a larger infrastructure and is not adapted for very constrained environments.

4.2. Surface vapor–precipitation isotopic relationships at the event scale

4.2.1 Comparison with outputs of LMDZ6-iso simulations

As previously shown in Dutrievoz et al., 2025 and Leroy-Dos Santos et al., 2023 modelling the isotopic composition of water vapor and precipitation at Dumont d'Urville (DDU) is particularly challenging due to the combined influence of both oceanic and continental processes. Over the ocean, isotopic variability is largely driven by evaporation, which itself depends on sea ice coverage. Over land, katabatic winds can affect both humidity and isotopic composition. Here, we evaluate the performance of the isotope-enabled global atmospheric model LMDZ6-iso nudged to the ERA5 reanalysis (same simulation as in (Dutrievoz et al., 2025)) with our new precipitation isotope dataset on the three case studies presented in Sect. 2.1. Although DDU lies at the boundary between an oceanic and a continental grid cell in LMDZ, the continental grid has an average altitude of 1032 m above sea level making it less adapted to describe surface water vapor isotopes at DDU (situated at a few meters above sea level). We will therefore compare observations with model outputs from the ocean grid cell in the following section (Figure 7).

Consistent with findings from (Dutrievoz et al., 2025) focused on December 2019, the model outputs on the ocean-grid cell show a positive bias in both humidity and δD_v compared to observations. However, the humidity bias appears to decrease for case 2 and get closer to zero for case 3 (winter conditions). For the three cases, the ocean grid cell does not reproduce well the intra-event variability of δD in vapor, with simulations often showing a too smoothed evolution. Interestingly, the simulated δD_p shows a close match with the observed δD_p, both in terms of absolute values and variability, although some deviations can be noted, such as during April 17th. This better match with δD_p could indicate that surface vapor isotopic signals are dominated by boundary-layer processes that are challenging to represent at the model resolution, while precipitation isotopes during the three events are mainly controlled by large-scale moisture transport and conditions during condensation at higher altitudes. These preliminary results suggest that δD in precipitation (δD_p), now available at high temporal resolution thanks to our method, may provide a new direct constraint on atmospheric processes, in particular to study the various processes from snow formation in the clouds to subsequent sublimation and interaction with the surface.

https://doi.org/10.5194/egusphere-2026-256
Preprint. Discussion started: 2 March 2026

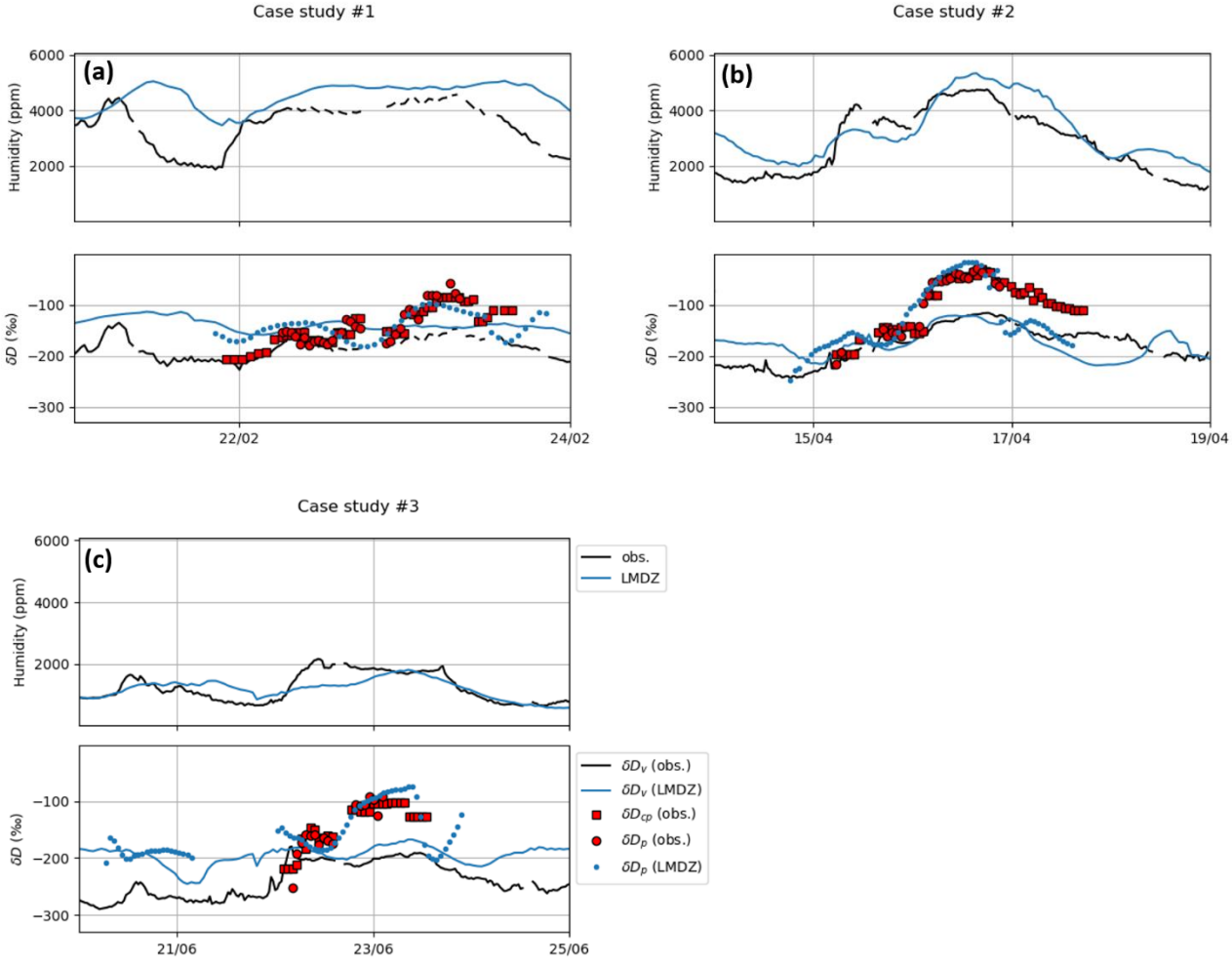

Figure 7: Comparison of LMDZ6iso model outputs with observations for case studies 1–3 (a–c). Top panels: absolute humidity. Bottom panels: δD. Solid lines correspond to vapor data (blue : LMDZ6iso ocean grid cell outputs, black : observations); markers correspond to precipitation (blue dots : LMDZ6iso outputs for precipitation above 10^{-4} kg.s^{-1}.m^{-2}, red circles and squares : online and manually collected samples, respectively).

4.2.2 Comparison with remote sensing observations

We further investigate the link between water vapor and precipitation isotopic composition by comparing δD_v with the theoretical equilibrium vapor $\delta D_{p,eq}$ derived from precipitation (represented with dark blue dots and horizontal lines in Figure 4 from section 3.1). This theoretical equilibrium vapor is obtained by calculating the equilibrium fractionation coefficient of vapor to solid phase transition $\alpha_{eq}(T)$ (Merlivat and Nief, 1967) at the ground temperature T (provided by Météo France weather station), with the following definition: $\delta D_{p,eq} = (\delta D_p+1)/\alpha_{eq}(T)-1$.

https://doi.org/10.5194/egusphere-2026-256
Preprint. Discussion started: 2 March 2026

Under a few assumptions, $\delta D_{p,eq}$ can provide a first-order estimate of the isotopic composition of the surrounding vapor during snow formation: 1/ snow forms above the observation site under thermodynamic equilibrium, with vapor deposition as the dominant growth process and 2/ once formed, snow falls directly to the surface without isotopic modification during descent. Within this idealized framework, the metric $\Delta(\delta D) = \delta D_{p,eq} - \delta D_v$ (Graf et al., 2019; Weng et al., 2021) can be interpreted as an indicator of the temperature or altitude difference between the surface and the level of snow formation, provided that the vertical isotopic gradient remains approximately constant. To test this hypothesis, we propose here to compare on Figure 8 the $\Delta(\delta D)$ metric from our new dataset to remote sensing observations from the CALVA program, including ceilometer-derived cloud base heights (CBH) and radar reflectivity data from a micro rain radar (Wiener et al., 2024). We focus below on case study 2, which is associated with the longest precipitation record (approximately 60 hours).

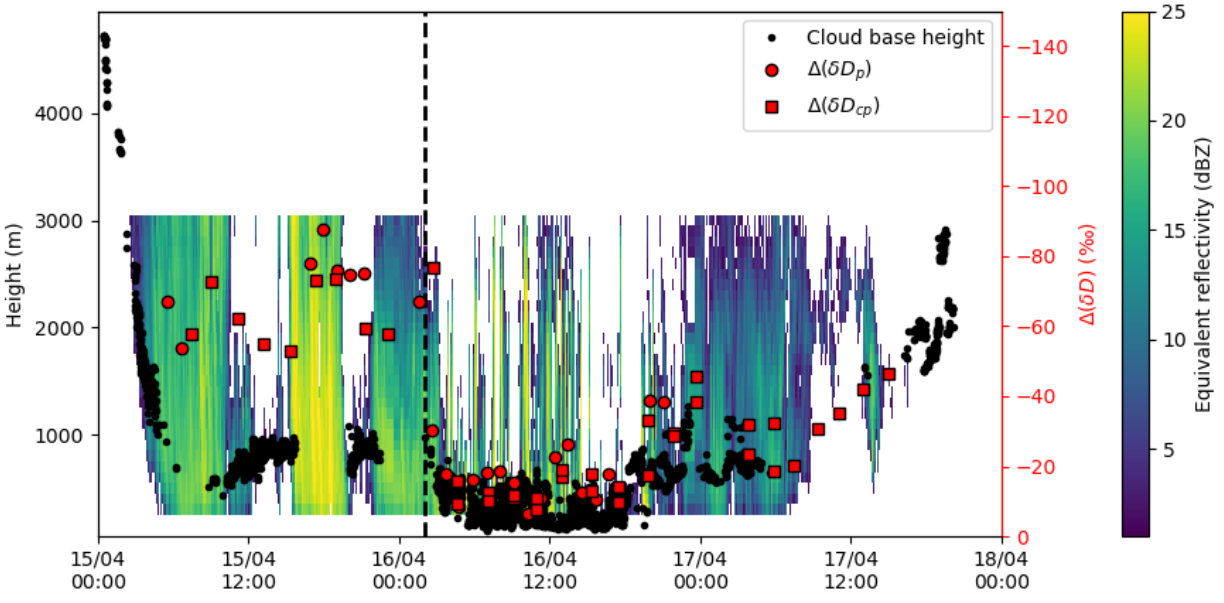

Figure 8: Combined view of in-situ isotope observations and remote sensing. Red circles (resp. squares) correspond to the Δ(δD) calculated from online (resp. collected) precipitation; the black dots correspond to the ceilometer-derived cloud base height and the MRR equivalent reflectivity is plotted in background (color scale). Note that the Δ(δD) axis is plotted on a reversed scale. The vertical dashed line separates the first and second parts of the event, situated on April 16th at 03:00 UTC.

On April 15th, periods of high reflectivity coincide with missing CBH data, indicating ceilometer signal attenuation due to intense precipitation. A sharp descent of the cloud base is observed from ~4 km at 01:00 UTC to below 1 km, stabilizing between 12:00 UTC and early April 16th, before descending to near-surface levels between 04:00 and 17:00 UTC. It then rises to ~850 m and then increases to ~2 km by 16:00 UTC, coinciding with the end of collected snow samples. Notably, two periods can be highlighted in Figure 8: a first part occurring in April 15th before the cloud descent to ground level with low values of $\Delta(\delta D)$, and a second part from April 16th at 03:00 UTC (indicated by the vertical dashed line in Figure 8) onward, where the $\Delta(\delta D)$ metric shows a consistent correlation with cloud base height.

https://doi.org/10.5194/egusphere-2026-256
Preprint. Discussion started: 2 March 2026

In the first part of the event, from April 15th to before 03:00 UTC on April 16th, Δ(δD) shows much lower values, around ~ -65 ‰ with a large variability. During this period, the MRR mostly shows high reflectivity values (10-20 dBZ) extending from the surface up to 3 km, with cloud tops exceeding the radar's observational range, indicating that snow particles likely originate from high altitudes. Two local maxima in Δ(δD) are observed on April 15th at approximately 14:00 and 20:00 UTC, each showing an increase of ~ +20 ‰ (note that the Δ(δD) y-axis is inverted, with higher values at the bottom). These maxima coincide with periods when almost no MRR signal is detected, although a delay in the hourly range is observed between the reflectivity gaps and the corresponding Δ(δD) maxima. This delay may reflect the fall time of snow particles and supports the idea that the isotopic signal carries an information related to the altitude of snow formation.

In the second part of the event, following the descent of the cloud base after 03:00 UTC on April 16th, maximum reflectivity remains below 3 km and is confined to a narrower vertical layer. This more compact vertical structure is consistent with the closer correlation between Δ(δD) and the measured cloud base height compared to the first part of the event.

While the comparison between remote sensing and water isotopes seems to support that Δ(δD) could be used as an indicator of the altitude difference between the surface and the snow formation altitude, it is also associated with some limitations. On the remote sensing side, observations are limited by the range (3 km) and the limit of detection (1.14 dBZ, see (Wiener et al., 2024)) of the micro rain radar, limiting its ability to detect upper cloud layers or resolve fine microphysical structures. This restricts the comparison of the Δ(δD) metric against detailed cloud and precipitation profiles, in particular during the first part of the event. In contrast, the use of cloud radars with higher sensitivity and range, and advanced capabilities (e.g. multifrequency, scanning, or polarimetric measurements) could provide more detailed insights into microphysical processes, including the vertical extent of vapor deposition and riming regions (Planat et al., 2021). From an isotopic perspective, one key assumption is that the fractionation coefficient used to retrieve $\delta D_{p,eq}$ and thus the ΔδD metric is based on surface temperature, although the precipitation is formed in altitude at significantly lower temperatures. In addition, in case of snow formation in high level clouds, a time delay is expected between the measurement of the isotopic composition of precipitation at ground level and the remote sensing data characterizing clouds in altitude. Using the Δ(δD) metric as a proxy for snow formation altitude may thus introduce biases when the cloud extent exceeds few km such as observed in the first part of the event. Finally, the Δ(δD) approach assumes equilibrium fractionation from vapor deposition and does not account for kinetic effects, such as supersaturation, mixing, rimed ice growth or snow sublimation. These processes can alter the isotopic signal of precipitation and contribute to variability in Δ(δD).

5. Conclusion and perspective

We have developed and validated a novel method for online measurement of precipitation isotopic composition using a single laser spectrometer, capable of analyzing both water vapor and solid precipitation. The method was tested across three precipitation events with a wide range of humidity conditions (~500-5000 ppm), representative of year-round variability on

https://doi.org/10.5194/egusphere-2026-256
Preprint. Discussion started: 2 March 2026

the East-Antarctica coast (Dumont d'Urville station). Comparisons with manually collected snow samples show a mean deviation of -5.4 ‰ in δD and a dispersion of 8.2 ‰, which we attribute mainly to calibration uncertainties and differences in the sampling frequency between online measurement and manual collection. Given that the observed intra-event variability of precipitation δD is on the order of 100 ‰, these uncertainties do not limit the signal interpretation. Compared to manual collection, the automated approach offers clear advantages: it requires no human intervention and is sensitive enough to detect very small precipitation volumes, making it well-suited for deployment in the low-precipitation environments of the Antarctic plateau.

Several technical improvements are foreseen, including the development of an orientable inlet and adjustable diaphragm to increase the likelihood of capturing snowflakes. Future efforts will also focus on enabling measurements of second-order isotopic parameters such as d-excess, which was not achievable with the current AP2E spectrometer setup.

We then illustrated two potential applications of this sampling method using our new dataset, representative of coastal regions of East-Antarctica. First, it can be used to better evaluate and constrain isotope-enabled atmospheric models such as LMDZiso for the isotopic composition of falling precipitation before its integration in the snowpack. This opens up new possibilities for evaluating the implementation of cloud processes and their impact on the isotopic composition of precipitation, for improving the representation of interactions between snowflakes and the atmosphere (particularly during sublimation), and for differentiating between drifting and falling snow. Second, we explored the relationship between surface water vapor and precipitation isotopic composition, and in particular the Δ(δD) metric, as a way to gain insight into snow formation conditions. Its comparison with ceilometer and micro rain radar observations revealed a promising correlation with cloud-base height, indicating that Δ(δD) could help identify key cloud processes such as the altitude of condensation. At this stage, the synergy between Δ(δD) and remote sensing remains limited both by the simplified assumptions underlying the metric and by the restricted vertical range and sensitivity of the micro rain radar. Ongoing deployments will help overcome some of these limitations. For example, the use of polarimetric radars (Planat et al., 2021) or multi-frequency remote sensing (Aubry et al., 2024; Billault-Roux et al., 2023) will allow for more detailed diagnosis of cloud microphysical structure and associated processes.

Finally, over the Antarctic plateau, where post-depositional sublimation strongly alters the surface signal, this technique provides a unique opportunity to directly quantify the isotopic composition of precipitation, even during low-intensity events typically missed by manual sampling. This will improve constraints on the primary isotopic signal and the reliability of ice core climate reconstructions.

Competing interests. The authors declare that they have no competing interests.

https://doi.org/10.5194/egusphere-2026-256
Preprint. Discussion started: 2 March 2026

Acknowledgments. We thank the logistics staff from the French Polar Institute (IPEV) at Dumont d'Urville Station, as well as the winterover Arnaud Reboud for the snow collection all over the year 2023, instrumental calibration and help with the data acquisition in the field. We thank Météo-France for providing the data from the meteorological station at DDU. We thank the CALVA and GLACIOCLIM IPEV programs for supporting the remote sensing instrumentation used in this study. We also indicate we used artificial intelligence (AI) tools to improve the English syntax in some sections of the manuscript, as well as for optimizing portions of the code.

Financial support. This research was supported by the IPEV ADELISE project (project no. 1205) and has received funding from the European Research Council (ERC) under the European Union's Horizon 2020 research and innovation programme (AWACA grant agreement no. 951596).

Author contributions. TL designed the study, the instrumental setup and the precipitation isotopes retrieval algorithm. TL optimised and calibrated the spectrometer, produced all the plots, and designed and wrote all sections of the original paper, with inputs from co-authors regarding revisions to the text. TL and EF installed the spectrometer and the snow collection system at DDU during the season 2022–2023. EF and AL made substantial contributions throughout the paper. TL, FP, OJ and OC fabricated and designed the online snow collection and vaporization system. BM performed the snow samples measurements in the lab. ND and CA made the simulations and provided the modelled isotopic data. OJ improved the software to control and adapt the valve switching system for snowflake measurements. VMD (PI of the ERC Synergy AWACA project) and AL designed the water isotopes section of the AWACA project. CG is PI of the ERC Synergy AWACA project, initiated the CALVA program and provided the remote sensing data.

References

Affolter, S., Fleitmann, D., and Leuenberger, M.: New online method for water isotope analysis of speleothem fluid inclusions using laser absorption spectroscopy (WS-CRDS), Clim. Past, 10, 1291–1304, https://doi.org/10.5194/cp-10-1291-2014, 2014.

Aubry, C., Delanoë, J., Groß, S., Ewald, F., Tridon, F., Jourdan, O., and Mioche, G.: Lidar–radar synergistic method to retrieve ice, supercooled water and mixed-phase cloud properties, Atmospheric Measurement Techniques, 17, 3863–3881, https://doi.org/10.5194/amt-17-3863-2024, 2024.

Bagheri Dastgerdi, S., Behrens, M., Bonne, J.-L., Hörhold, M., Lohmann, G., Schlosser, E., and Werner, M.: Continuous monitoring of surface water vapour isotopic compositions at Neumayer Station III, East Antarctica, The Cryosphere, 15, 4745–4767, https://doi.org/10.5194/tc-15-4745-2021, 2021.

Billault-Roux, A.-C., Ghiggi, G., Jaffeux, L., Martini, A., Viltard, N., and Berne, A.: Dual-frequency spectral radar retrieval of snowfall microphysics: a physics-driven deep-learning approach, Atmospheric Measurement Techniques, 16, 911–940, https://doi.org/10.5194/amt-16-911-2023, 2023.

https://doi.org/10.5194/egusphere-2026-256
Preprint. Discussion started: 2 March 2026

Bonne, J.-L., Behrens, M., Meyer, H., Kipfstuhl, S., Rabe, B., Schönicke, L., Steen-Larsen, H. C., and Werner, M.: Resolving the controls of water vapour isotopes in the Atlantic sector, Nat Commun, 10, 1632, https://doi.org/10.1038/s41467-019-09242-6, 2019.

Dansgaard, W.: The O18-abundance in fresh water, Geochimica et Cosmochimica Acta, 6, 241–260, https://doi.org/10.1016/0016-7037(54)90003-4, 1954.

Dansgaard, W.: Stable isotopes in precipitation, Tellus, 16, 436–468, https://doi.org/10.1111/j.2153-3490.1964.tb00181.x, 1964.

Dansgaard, W., Nief, G., and Roth, E.: Isotopic Distribution in a Greenland Iceberg, Nature, 185, 232–232, https://doi.org/10.1038/185232a0, 1960.

Del Guasta, M.: ICE-CAMERA: a flatbed scanner to study inland Antarctic polar precipitation, Atmospheric Measurement Techniques, 15, 6521–6544, https://doi.org/10.5194/amt-15-6521-2022, 2022.

Dreossi, G., Masiol, M., Stenni, B., Zannoni, D., Scarchilli, C., Ciardini, V., Casado, M., Landais, A., Werner, M., Cauquoin, A., Casasanta, G., Del Guasta, M., Posocco, V., and Barbante, C.: A decade (2008–2017) of water stable isotope composition of precipitation at Concordia Station, East Antarctica, The Cryosphere, 18, 3911–3931, https://doi.org/10.5194/tc-18-3911-2024, 2024.

Dutrievoz, N., Agosta, C., Risi, C., Vignon, É., Nguyen, S., Landais, A., Fourré, E., Leroy, C., Santos, D., Casado, M., Masson, V., Jouzel, J., Dubos, T., Ollivier, I., Stenni, B., Dreossi, G., Masiol, M., Minster, B., and Prié, F.: Antarctic Water Stable Isotopes in the Global Atmospheric Model LMDZ6: From Climatology to Boundary Layer Processes, Journal of Geophysical Research, 2025.

Dütsch, M., Pfahl, S., and Wernli, H.: Drivers of δ2H variations in an idealized extratropical cyclone, Geophysical Research Letters, 43, 5401–5408, https://doi.org/10.1002/2016GL068600, 2016.

Ehhalt, D., Knott, K., Nagel, J. F., and Vogel, J. C.: Deuterium and oxygen 18 in rain water, Journal of Geophysical Research (1896-1977), 68, 3775–3780, https://doi.org/10.1029/JZ068i013p03775, 1963.

Emanuelsson, B. D., Thomas, E. R., Tetzner, D. R., Humby, J. D., and Vladimirova, D. O.: Ice Core Chronologies from the Antarctic Peninsula: The Palmer, Jurassic, and Rendezvous Age-Scales, Geosciences, 12, 87, https://doi.org/10.3390/geosciences12020087, 2022.

Gonfiantini, R. and Picciotto, E.: Oxygen Isotope Variations in Antarctic Snow Samples, Nature, 184, 1557–1558, https://doi.org/10.1038/1841557a0, 1959.

González, Y., Schneider, M., Dyroff, C., Rodríguez, S., Christner, E., García, O. E., Cuevas, E., Bustos, J. J., Ramos, R., Guirado-Fuentes, C., Barthlott, S., Wiegele, A., and Sepúlveda, E.: Detecting moisture transport pathways to the subtropical North Atlantic free troposphere using paired H_2O-δD in situ measurements, Atmospheric Chemistry and Physics, 16, 4251–4269, https://doi.org/10.5194/acp-16-4251-2016, 2016.

Graf, P., Wernli, H., Pfahl, S., and Sodemann, H.: A new interpretative framework for below-cloud effects on stable water isotopes in vapour and rain, Atmos. Chem. Phys., 2019.

Grisart, A., Casado, M., Gkinis, V., Vinther, B., Naveau, P., Vrac, M., Laepple, T., Minster, B., Prié, F., Stenni, B., Fourré, E., Steen-Larsen, H. C., Jouzel, J., Werner, M., Pol, K., Masson-Delmotte, V., Hoerhold, M., Popp, T., and Landais, A.: Sub-

millennial climate variability from high-resolution water isotopes in the EPICA Dome C ice core, Climate of the Past, 18, 2289–2301, https://doi.org/10.5194/cp-18-2289-2022, 2022.

Guilpart, E., Vimeux, F., Evan, S., Brioude, J., Metzger, J.-M., Barthe, C., Risi, C., and Cattani, O.: The isotopic composition of near-surface water vapor at the Maïdo observatory (Reunion Island, southwestern Indian Ocean) documents the controls of the humidity of the subtropical troposphere, Journal of Geophysical Research: Atmospheres, 122, 9628, https://doi.org/10.1002/2017JD026791, 2017.

Jones, T. R., Cuffey, K. M., Roberts, W. H. G., Markle, B. R., Steig, E. J., Stevens, C. M., Valdes, P. J., Fudge, T. J., Sigl, M., Hughes, A. G., Morris, V., Vaughn, B. H., Garland, J., Vinther, B. M., Rozmiarek, K. S., Brashear, C. A., and White, J. W. C.: Seasonal temperatures in West Antarctica during the Holocene, Nature, 613, 292–297, https://doi.org/10.1038/s41586-022-05411-8, 2023.

Jouzel, J., Masson-Delmotte, V., Cattani, O., Dreyfus, G., Falourd, S., Hoffmann, G., Minster, B., Nouet, J., Barnola, J. M., Chappellaz, J., Fischer, H., Gallet, J. C., Johnsen, S., Leuenberger, M., Loulergue, L., Luethi, D., Oerter, H., Parrenin, F., Raisbeck, G., Raynaud, D., Schilt, A., Schwander, J., Selmo, E., Souchez, R., Spahni, R., Stauffer, B., Steffensen, J. P., Stenni, B., Stocker, T. F., Tison, J. L., Werner, M., and Wolff, E. W.: Orbital and Millennial Antarctic Climate Variability over the Past 800,000 Years, Science, 317, 793–796, https://doi.org/10.1126/science.1141038, 2007.

Jouzel, J., Delaygue, G., Landais, A., Masson-Delmotte, V., Risi, C., and Vimeux, F.: Water isotopes as tools to document oceanic sources of precipitation, Water Resources Research, 49, 7469–7486, https://doi.org/10.1002/2013WR013508, 2013.

Landais, A., Agosta, C., Vimeux, F., Magand, O., Solis, C., Cauquoin, A., Dutrievoz, N., Risi, C., Leroy-Dos Santos, C., Fourré, E., Cattani, O., Jossoud, O., Minster, B., Prié, F., Casado, M., Dommergue, A., Bertrand, Y., and Werner, M.: Abrupt excursions in water vapor isotopic variability at the Pointe Benedicte observatory on Amsterdam Island, Atmospheric Chemistry and Physics, 24, 4611–4634, https://doi.org/10.5194/acp-24-4611-2024, 2024.

Lauwers, T., Fourré, E., Jossoud, O., Romanini, D., Prié, F., Nitti, G., Casado, M., Jaulin, K., Miltner, M., Farradèche, M., Masson-Delmotte, V., and Landais, A.: OF–CEAS laser spectroscopy to measure water isotopes in dry environments: example of application in Antarctica, Atmospheric Measurement Techniques, 18, 1135–1147, https://doi.org/10.5194/amt-18-1135-2025, 2025.

Leinonen, J., Grazioli, J., and Berne, A.: Reconstruction of the mass and geometry of snowfall particles from multi-angle snowflake camera (MASC) images, Atmospheric Measurement Techniques, 14, 6851–6866, https://doi.org/10.5194/amt-14-6851-2021, 2021.

Leroy-Dos Santos, C., Casado, M., Prié, F., Jossoud, O., Kerstel, E., Kassi, S., Fourré, E., and Landais, A.: A dedicated robust instrument for water vapor generation at low humidity for use with a laser waterisotope analyzer in cold and dry polar regions., Others (Wind, Precipitation, Temperature, etc.)/In Situ Measurement/Instruments and Platforms, https://doi.org/10.5194/amt-2020-345, 2020.

Leroy-Dos Santos, C., Casado, M., Prié, F., Jossoud, O., Kerstel, E., Farradèche, M., Kassi, S., Fourré, E., and Landais, A.: A dedicated robust instrument for water vapor generation at low humidity for use with a laser water isotope analyzer in cold and dry polar regions, Atmos. Meas. Tech., 14, 2907–2918, https://doi.org/10.5194/amt-14-2907-2021, 2021.

Leroy-Dos Santos, C., Fourré, E., Agosta, C., Casado, M., Cauquoin, A., Werner, M., Minster, B., Prié, F., Jossoud, O., Petit, L., and Landais, A.: From atmospheric water isotopes measurement to firn core interpretation in Adélie Land: a case study for isotope-enabled atmospheric models in Antarctica, The Cryosphere, 17, 5241–5254, https://doi.org/10.5194/tc-17-5241-2023, 2023.

https://doi.org/10.5194/egusphere-2026-256
Preprint. Discussion started: 2 March 2026

Lorius, C.: Concentration en deuterium des couches de névé dans I'Antarctique, Annales de Géophysique, 17, 378–387, 1961.

Lowenthal, D., Hallar, A. G., McCubbin, I., David, R., Borys, R., Blossey, P., Muhlbauer, A., Kuang, Z., and Moore, M.: Isotopic Fractionation in Wintertime Orographic Clouds, https://doi.org/10.1175/JTECH-D-15-0233.1, 2016.

Lowenthal, D. H., Borys, R. D., Cotton, W., Saleeby, S., Cohn, S. A., and Brown, W. O. J.: The altitude of snow growth by riming and vapor deposition in mixed-phase orographic clouds, Atmospheric Environment, 45, 519–522, https://doi.org/10.1016/j.atmosenv.2010.09.061, 2011.

Merlivat, L. and Nief, G.: Fractionnement isotopique lors des changements d'état solide-vapeur et liquide-vapeur de l'eau à des températures inférieures à 0°C, Tellus, 19, 122–127, https://doi.org/10.1111/j.2153-3490.1967.tb01465.x, 1967.

Muller, C. L., Baker, A., Fairchild, I. J., Kidd, C., and Boomer, I.: Intra-Event Trends in Stable Isotopes: Exploring Midlatitude Precipitation Using a Vertically Pointing Micro Rain Radar, Journal of Hydrometeorology, 16, 194–213, https://doi.org/10.1175/JHM-D-14-0038.1, 2015.

Noone, D., Galewsky, J., Sharp, Z. D., Worden, J., Barnes, J., Baer, D., Bailey, A., Brown, D. P., Christensen, L., Crosson, E., Dong, F., Hurley, J. V., Johnson, L. R., Strong, M., Toohey, D., Van Pelt, A., and Wright, J. S.: Properties of air mass mixing and humidity in the subtropics from measurements of the D/H isotope ratio of water vapor at the Mauna Loa Observatory, Journal of Geophysical Research: Atmospheres, 116, https://doi.org/10.1029/2011JD015773, 2011.

Ollivier, I., Steen-Larsen, H. C., Stenni, B., Arnaud, L., Casado, M., Cauquoin, A., Dreossi, G., Genthon, C., Minster, B., Picard, G., Werner, M., and Landais, A.: Surface processes and drivers of the snow water stable isotopic composition at Dome C, East Antarctica – a multi-dataset and modelling analysis, The Cryosphere, 19, 173–200, https://doi.org/10.5194/tc-19-173-2025, 2025a.

Ollivier, I., Lauwers, T., Dutrievoz, N., Agosta, C., Casado, M., Fourré, E., Genthon, C., Jossoud, O., Prié, F., Steen-Larsen, H. C., and Landais, A.: Time series of the summertime atmospheric water vapour isotopic composition at Concordia station, East Antarctica, Earth System Science Data, 17, 5655–5674, https://doi.org/10.5194/essd-17-5655-2025, 2025b.

Picciotto, E., De Maere, X., and Friedman, I.: Isotopic Composition and Temperature of Formation of Antarctic Snows, Nature, 187, 857–859, https://doi.org/10.1038/187857a0, 1960.

Piel, C., Romanini, D., Farradèche, M., Chaillot, J., Paul, C., Bienville, N., Lauwers, T., Sauze, J., Jaulin, K., Prié, F., and Landais, A.: High precision δ18O measurements of atmospheric dioxygen using optical-feedback cavity-enhanced absorption spectroscopy (OF-CEAS), Atmospheric Measurement Techniques Discussions, 1–22, https://doi.org/10.5194/amt-2024-14, 2024.

Planat, N., Gehring, J., Vignon, É., and Berne, A.: Identification of snowfall microphysical processes from Eulerian vertical gradients of polarimetric radar variables, Atmospheric Measurement Techniques, 14, 4543–4564, https://doi.org/10.5194/amt-14-4543-2021, 2021.

Pol, K., Masson-Delmotte, V., Cattani, O., Debret, M., Falourd, S., Jouzel, J., Landais, A., Minster, B., Mudelsee, M., Schulz, M., and Stenni, B.: Climate variability features of the last interglacial in the East Antarctic EPICA Dome C ice core, Geophysical Research Letters, 41, 4004–4012, https://doi.org/10.1002/2014GL059561, 2014.

Risi, C., Bony, S., Vimeux, F., and Jouzel, J.: Water-stable isotopes in the LMDZ4 general circulation model: Model evaluation for present-day and past climates and applications to climatic interpretations of tropical isotopic records, Journal of Geophysical Research: Atmospheres, 115, https://doi.org/10.1029/2009JD013255, 2010.

https://doi.org/10.5194/egusphere-2026-256
Preprint. Discussion started: 2 March 2026

590 Rozanski, K., Sonntag, C., and Münnich, K. O.: Factors controlling stable isotope composition of European precipitation, Tellus, 34, 142–150, https://doi.org/10.1111/j.2153-3490.1982.tb01801.x, 1982.

Schmidt, G. A., LeGrande, A. N., and Hoffmann, G.: Water isotope expressions of intrinsic and forced variability in a coupled ocean-atmosphere model, Journal of Geophysical Research: Atmospheres, 112, https://doi.org/10.1029/2006JD007781, 2007.

Steen-Larsen, H. C., Johnsen, S. J., Masson-Delmotte, V., Stenni, B., Risi, C., Sodemann, H., Balslev-Clausen, D., Blunier,
595 T., Dahl-Jensen, D., Ellehøj, M. D., Falourd, S., Grindsted, A., Gkinis, V., Jouzel, J., Popp, T., Sheldon, S., Simonsen, S. B., Sjolte, J., Steffensen, J. P., Sperlich, P., Sveinbjörnsdóttir, A. E., Vinther, B. M., and White, J. W. C.: Continuous monitoring of summer surface water vapor isotopic composition above the Greenland Ice Sheet, Atmospheric Chemistry and Physics, 13, 4815–4828, https://doi.org/10.5194/acp-13-4815-2013, 2013.

Wahl, S., Steen-Larsen, H. C., Reuder, J., and Hörhold, M.: Quantifying the Stable Water Isotopologue Exchange Between
600 the Snow Surface and Lower Atmosphere by Direct Flux Measurements, Journal of Geophysical Research: Atmospheres, 126, e2020JD034400, https://doi.org/10.1029/2020JD034400, 2021.

Weng, Y., Touzeau, A., and Sodemann, H.: Correcting the impact of the isotope composition on the mixing ratio dependency of water vapour isotope measurements with cavity ring-down spectrometers, Atmos. Meas. Tech., 13, 3167–3190, https://doi.org/10.5194/amt-13-3167-2020, 2020.

605 Weng, Y., Johannessen, A., and Sodemann, H.: High-resolution stable isotope signature of a land-falling atmospheric river in southern Norway, Weather and Climate Dynamics, 2, 713–737, https://doi.org/10.5194/wcd-2-713-2021, 2021.

Werner, M., Langebroek, P. M., Carlsen, T., Herold, M., and Lohmann, G.: Stable water isotopes in the ECHAM5 general circulation model: Toward high-resolution isotope modeling on a global scale, Journal of Geophysical Research: Atmospheres, 116, https://doi.org/10.1029/2011JD015681, 2011.

610 Wiener, V., Roussel, M.-L., Genthon, C., Vignon, É., Grazioli, J., and Berne, A.: A 7-year record of vertical profiles of radar measurements and precipitation estimates at Dumont d'Urville, Adélie Land, East Antarctica, Earth System Science Data, 16, 821–836, https://doi.org/10.5194/essd-16-821-2024, 2024.

Worden, J., Noone, D., and Bowman, K.: Importance of rain evaporation and continental convection in the tropical water cycle, Nature, 445, 528–532, https://doi.org/10.1038/nature05508, 2007.

615 Xing, M., Liu, W., Hu, J., and Wang, Z.: A set of methods to evaluate the below-cloud evaporation effect on local precipitation isotopic composition: a case study for Xi'an, China, Atmospheric Chemistry and Physics, 23, 9123–9136, https://doi.org/10.5194/acp-23-9123-2023, 2023.